

NASA/TM-2002-211420



Orbiter Cold Plate Intergranular Corrosion: Development of NDE Standards and Assessment of NDE Methods

*Stephen W. Smith, William P. Winfree, and Robert S. Piascik
Langley Research Center, Hampton, Virginia*

January 2002

The NASA STI Program Office . . . in Profile

Since its founding, NASA has been dedicated to the advancement of aeronautics and space science. The NASA Scientific and Technical Information (STI) Program Office plays a key part in helping NASA maintain this important role.

The NASA STI Program Office is operated by Langley Research Center, the lead center for NASA's scientific and technical information. The NASA STI Program Office provides access to the NASA STI Database, the largest collection of aeronautical and space science STI in the world. The Program Office is also NASA's institutional mechanism for disseminating the results of its research and development activities. These results are published by NASA in the NASA STI Report Series, which includes the following report types:

- TECHNICAL PUBLICATION. Reports of completed research or a major significant phase of research that present the results of NASA programs and include extensive data or theoretical analysis. Includes compilations of significant scientific and technical data and information deemed to be of continuing reference value. NASA counterpart of peer-reviewed formal professional papers, but having less stringent limitations on manuscript length and extent of graphic presentations.
- TECHNICAL MEMORANDUM. Scientific and technical findings that are preliminary or of specialized interest, e.g., quick release reports, working papers, and bibliographies that contain minimal annotation. Does not contain extensive analysis.
- CONTRACTOR REPORT. Scientific and technical findings by NASA-sponsored contractors and grantees.
- CONFERENCE PUBLICATION. Collected papers from scientific and technical conferences, symposia, seminars, or other meetings sponsored or co-sponsored by NASA.
- SPECIAL PUBLICATION. Scientific, technical, or historical information from NASA programs, projects, and missions, often concerned with subjects having substantial public interest.
- TECHNICAL TRANSLATION. English-language translations of foreign scientific and technical material pertinent to NASA's mission.

Specialized services that complement the STI Program Office's diverse offerings include creating custom thesauri, building customized databases, organizing and publishing research results . . . even providing videos.

For more information about the NASA STI Program Office, see the following:

- Access the NASA STI Program Home Page at <http://www.sti.nasa.gov>
- Email your question via the Internet to help@sti.nasa.gov
- Fax your question to the NASA STI Help Desk at (301) 621-0134
- Telephone the NASA STI Help Desk at (301) 621-0390
- Write to:
NASA STI Help Desk
NASA Center for AeroSpace Information
7121 Standard Drive
Hanover, MD 21076-1320

NASA/TM-2002-211420



Orbiter Cold Plate Intergranular Corrosion: Development of NDE Standards and Assessment of NDE Methods

*Stephen W. Smith, William P. Winfree, and Robert S. Piascik
Langley Research Center, Hampton, Virginia*

National Aeronautics and
Space Administration

Langley Research Center
Hampton, Virginia 23681-2199

January 2002

Available from:

NASA Center for AeroSpace Information (CASI)
7121 Standard Drive
Hanover, MD 21076-1320
(301) 621-0390

National Technical Information Service (NTIS)
5285 Port Royal Road
Springfield, VA 22161-2171
(703) 605-6000

Abstract

During pre-servicing of a space shuttle (orbiter vehicle, OV-102), helium leak detection of an avionics cold plate identified a leak located in the face sheet oriented towards the support shelf. Subsequent destructive examination of the leaking cold plate revealed that intergranular corrosion had penetrated the 0.017-inch thick aluminum (AA6061) face sheet. The intergranular attack (IGA) was likely caused by an aggressive crevice environment created by condensation of water vapor between the cold plate and support shelf. Face sheet susceptibility to IGA is a result of the brazing process used in the fabrication of the cold plates. Cold plate components were brazed at 1000°F followed by a slow cooling process to avoid distortion of the bonded cold plate. The slow cool process caused excessive grain boundary precipitation resulting in a material that is susceptible to IGA. The objectives of this work are as follows:

(1) Develop first-of-a-kind NDE standards that contain IGA similar to that found in the orbiter cold plates.

(2) Assess advanced NDE techniques for corrosion detection and recommend methods for cold plate examination.

This report documents the results of work performed at LaRC to fulfill these objectives.

Procedures

Accelerated Corrosion Method:

Test specimens and NDE standards (1 inch by 1 inch) were machined from a cold plate¹ supplied by JSC and prepared in the following manner. One face of the specimen was polished (thru 600 grit) to remove the protective chromate film applied during manufacture and to expose the bare face sheet material. All specimen surfaces, except for the polished face sheet region, were masked with a corrosion protective wax. Specimens were electrically coupled to a cathode (steel coupon) and immersed in a mild electrolyte solution (20 mM - NaCl, 4mM - NaNO₂, 4 mM - NaHCO₃, 2 mM - NaF). The cathode was used to supply a corrosion current to the 1 square inch anode (polished cold plate surface) and thus accelerate the intergranular corrosion. A series of preliminary electrochemical experiments were performed; here, the surface area of the cathode and the exposure time were varied until the optimum amount of IGA was produced in the exposed face sheet. Two different cathodes were used, a 1-1/2-inch by 1-1/2-inch and a 2-1/4-inch by 2-1/4-inch steel electrode. By changing the exposed surface area of the cathode, the applied corrosion current was varied. When coupled to the 1-1/2-inch by 1-1/2-inch cathode, the electrochemical potential of the cold plate specimens was \approx -600 mV versus a saturated calomel electrode (SCE). Exposure time was varied between 8 and 30 hours. Table 1, Part A summarizes the corrosion testing.

¹ The cold plate was removed from Orbiter OV-102. The cold plate passed a helium leak detection procedure and visual inspection detected no evidence of corrosion.

Destructive Examination Procedure:

Destructive examination results were used to qualify the laboratory IGA corrosion test method and the CT radiography method (described below). To accurately characterize the IGA produced by the laboratory test method, specimens were metallographically sectioned through the thickness, mounted edge-on in epoxy, polished and examined using an optical microscope. Selected regions containing IGA were examined in great detail; here, multiple metallographic sections at 0.004 to 0.008-inch intervals were performed to accurately characterize the corrosion events. Each metallographic section was examined at high magnification to determine the maximum IGA depth, width and position. Table 1, Part B summarizes the destructive examinations conducted.

Nondestructive Evaluation Techniques:

NDE methods were evaluated based on their ability to detect IGA in the corrosion standards. The NDE methods used to examine the corroded cold plate specimens (standards) included, immersion ultrasonics, laser ultrasonics, eddy current, thermography, and digital radiography. CT radiography (qualified by the destructive examination procedure) was used to fully characterize each IGA corrosion standard prior to using the five NDE methods. Past experience at NASA-LaRC has shown that CT radiography is a valuable tool and is used herein to conduct a three-dimensional characterization of the IGA contained in each standard. Two restrictions were placed on all NDE testing; all specimens were limited to a 1 inch by 1 inch size, which is the maximum size that can be examined with the CT radiography system at NASA-LaRC, and all immersion ultrasonic measurements were conducted by placing the specimens in methanol instead of water to avoid further corrosion damage. Table 1, Part C lists the number of NDE tests conducted.

CT Radiography (Microfocus X-ray Computed Tomography): Computed tomography was performed with a microfocus CT system. The microfocus x-ray source is 160 kV with a 0.002-inch spot size. The detector package contains 8192 separate detectors with 0.001-inch center separation and was positioned approximately 40 inches from the source. The specimen was mounted on a rotation stage and was centered between the source and detector. Geometric constraints limit the field of view of the system in the horizontal plane to a circle approximately 3.5 inches in diameter. The x-ray attenuation of aluminum was the limiting factor for measurements in these specimens. Specimens were limited to 1 inch by 1 inch to obtain a reasonable signal to noise ratio when using the 160 kV source.

Data were acquired every 0.1 degrees of rotation for each specimen to obtain the required information for computed reconstruction of the density for a specimen cross-section. At each rotation angle, the data were acquired by integrating the response of the detectors for 10 seconds. Including data transfer time, the total time required to acquire a single cross section was approximately 11 hours.

The microfocus x-ray system was capable of generating images with voxels 0.0005 inch by 0.0005 inch with a vertical height of 0.004 inch. For such images, resolution in the horizontal plane was 0.0025 inch by 0.0025 inch. The rotation stage was mounted on a vertical positioning stage; the position of the vertical stage specifies the portion of the depth into the specimen that will be imaged. A series of images with different mean sampling depths were acquired by moving the vertical stage in steps of 0.002 inch. This results in overlaps of 50% between data sets.

Immersion Ultrasonics: To ensure that the face-sheet portion of the specimen was placed at the

proper transducer focal length, a thin wire was placed on the surface of each specimen before performing any measurements. A sharp image of the wire was acquired by adjusting the vertical position of the transducer above the specimen. The 20 MHz focused transducer was scanned above the specimen surface and the ultrasonic response was recorded digitally. The transducer was scanned over the area in 0.01-inch increments. At each position, the transducer was excited with a short, broadband electronic pulse, which produces a broadband ultrasonic wave that propagates to the specimen. The echo of the sound wave was measured with the same transducer. This measurement was digitized at 100 MHz and recorded for post processing. The digitization was triggered by a signal corresponding to the echo off the front surface of the specimen. The digitizer was configured to enable capture and digitization of the output of the transducer both before and after the trigger is received.

Laser Ultrasonics: Laser ultrasonics is similar to immersion ultrasonics in that both characterize the ultrasonic response of a specimen. However, laser ultrasonics has a significant advantage since it requires no physical couplant, with all the measurement being performed optically. Laser ultrasonics also has a significant disadvantage in that it is orders of magnitude less sensitive. Additionally, the methods of generation are significantly different and produce different modes of ultrasonic propagation. Therefore, each technique can render significantly different kinds of information about the specimen.

For laser ultrasonics measurements, a 1064 nm line from a pulsed Nd:YAG laser was used as the excitation pulse. The beam diameter was 0.120 inch, with an energy of approximately 20 mJ per pulse. The ultrasonic response was measured by reflecting a 532 nm line from a continuous wave Nd:YAG laser into a Fabry-Perot interferometer. The diameter of the detecting beam was 0.080 inch with a power of 400 mW. The interferometer output, which is a function of the ultrasonic response, was recorded digitally at 100 MHz for post processing.

The specimen was mounted in front of the measurement system on a vertical and horizontal translation stage. The specimen was moved in 0.025-inch horizontal and vertical increments to measure the response for the entire surface of the specimen.

Eddy Current: For the eddy current characterization of a specimen, the specimen was mounted on a scanning table and inspected in air. A special eddy current probe (a self-nulling probe developed at LaRC) was scanned above the surface. The probe was sensitive to the edges of the specimen; therefore, only a 0.5-inch by 0.5-inch region in the center of the specimen was analyzed by scanning the probe in 0.01-inch increments. The probe diameter was approximately 0.04 inch. The probe was operated at 100 kHz and 200 kHz, with 200 kHz being more sensitive to near surface variations in the conductivity and 100 kHz characterizing about 1.4 times deeper into the specimen.

Thermography: For thermal inspections of structures, the surface emissivity must be sufficiently high such that the infrared radiation from the surface is indicative of the temperature of the surface rather than a reflection of background radiation. A thin coat of flat paint is conventionally used as a good emissivity coating with insignificant spatial variations. Initial measurements were performed with a thin coat of lacquer paint on the surface. Due to the thinness of the aluminum face sheet, this coating proved to be too great of a thermal barrier and significantly impacted the thermal response of the specimen. Several other coatings were attempted. The coating that produced the best results was black magic marker thinned with alcohol. This coating was used for the measurements presented.

The thermographic technique involves heating a specimen and measuring its thermal response. The specimen was heated by two xenon flash lamps placed on opposite sides of the specimen. They were fired to give a short pulse of light that heats the front surface of the specimen. The duration of the light

pulse was approximately 2 milliseconds. An infrared imager with a cooled 256 by 256-element InSb focal plane array detector was used to characterize the variations in surface temperature. The detector operates in the 3 to 5 micrometer wavelength range. The imaging radiometer produces 1500 frames per second in a 12-bit digital signal, which was input into a computer using an RS422 interface. The first 0.08 seconds of the thermal response following the flash were recorded for later analysis. An external close-up lens was positioned to image an area of approximately 0.1 by 0.1 inch. For purposes of scanning a 1 by 1-inch specimen, the specimen was mounted on a positioning stage that was capable of translating the specimen both vertically and horizontally.

Digital Radiography: Digital radiography was performed with a scanned x-ray source system. The specimen was placed on the source, and the variations in x-ray intensity, as a function of position on the specimen, were measured with a NaI (TI) scintillator coupled to a photomultiplier. Spatial resolution of the system was 0.03 inch for inspection of a specimen area up to 7 inches by 7 inches. Images were obtained for two acceleration voltages (100 kV and 120 kV) and compared to determine if the difference in energy dependence of the attenuation between aluminum and oxygen would enhance the visualization of corrosion products. The x-ray intensities were digitally recorded. Post processing of the images was performed to identify and enhance variations between corroded and noncorroded regions.

Results

Fabrication of NDE Standards:

Destructive Examination (Metallography): Initial destructive examinations were performed on corroded cold plate samples to evaluate the morphology of the IGA and to compare these results with the IGA observed in cold plates removed from the orbiter. Figure 1 contains a series of optical micrographs for a corroded sample that was exposed to the electrolyte solution for 24 hours, sectioned and polished. Several discreet corrosion events, identified by small white arrows in Figure 1, are identified along each section. Here, the 1-inch by 1-inch cold plate sample was coupled to a 1-1/2-inch by 1-1/2-inch steel cathode and immersed in the electrolyte. The resultant IGA was very similar to that observed for in-service cold plates. When a 2-1/4-inch by 2-1/4-inch steel cathode was used, excessive pitting, which was not present for the in-service cold plates, was produced. Therefore, all corroded cold plate specimens used for NDE evaluation were fabricated by coupling to a 1-1/2-inch by 1-1/2-inch steel cathode. For each event, a maximum penetration depth and width were recorded (see Figure 1c). Such measurements were performed for several specimens exposed to the electrolyte solution for various times. Figure 2 shows results of depth versus width of IGA for three specimens exposed to the electrolyte for 8 hours (Figure 2a) and three specimens exposed for 24 hours (Figure 2b). Each specimen was polished six times, to examine six different cross-sections. Microscopic measurements of width, depth and position for all IGA events were performed on each metallographic section, to provide an accurate assessment of the IGA events. As can be seen in Figure 2, the average depth and width for the observed IGA was greater when the cold plate samples were exposed to the solution for 24 hours (See Figure 2b.) than when they were exposed for 8 hours (See Figure 2a.). To ensure that the NDE standards contained a wide distribution of IGA events, two NDE standard types (24 hour and 8 hour electrolyte exposure) were produced.

CT Radiography: To validate CT radiography results, metallography was performed to confirm IGA corrosion depth measurements. CT images of a corroded (24 hour) specimen face sheet were acquired at 0.002-inch increments. Figures 3 – 8 show the CT radiography results for mean sampling depths of 0.0035, 0.0055, 0.0075, 0.0095, 0.115 and 0.0135-inch, respectively. Each figure shows a radiographic

image where the dark gray areas indicate localized regions of IGA corrosion. In the second image of each figure (Figures 3b – 7b), these localized IGA events have been artificially darkened and outlined in white for ease of identification. Because discreet depth images were produced, a mean maximum depth was determined for each IGA corrosion event. For example, a region is identified in each radiograph as site A (see Figures 3b – 7b). Here, a corrosion event was observed at this site for the 0.0035 and 0.0055-inch images (Figures 3 and 4) and was not observed at a depth of 0.0075-inch and greater (Figures 5 – 7). For this example, a mean maximum IGA depth of 0.0065-inch was determined for this event. Similarly, an IGA event would be determined to have a mean maximum depth of 0.0045-inch if it was identified at a depth of 0.0035-inch and not observed at the 0.0055-inch depth. If an event were identified in only one CT image, the event would be discarded from further consideration.

Two additional corroded (24 hour) specimens were examined to determine the accuracy of the CT radiography system in measuring IGA. The CT radiographic inspections were conducted at the same depths described above; thus categorizing the IGA events at mean maximum corrosion depths of 0.0045, 0.0065, 0.0085, 0.0105 or 0.0125 inch. After CT radiography of the two corroded specimens was completed, a total of 32 metallographic cross-sections were microscopically examined. Each IGA corrosion event was characterized for depth, width and location and compared to the CT radiography results. Figure 9 is a plot of the mean maximum depth for 27 IGA events determined by CT radiography versus the maximum depth of the same events determined by the destructive examinations. Table 2 summarizes the statistical analysis of the data presented in Figure 9. A 95% confidence interval was determined for CT radiography results at the 0.0065, 0.0085, and 0.0105 inch mean maximum depths. If CT radiography indicates that an IGA event is 0.0105 inch deep, there is a 95% certainty that the event is between 0.0086 and 0.0122 inch in depth. Due to a lack of data, it was not possible to determine confidence intervals for CT results less than 0.0065 inch and greater than 0.0105 inch. Based on these results, the CT radiographic method was used to fully characterize the IGA corrosion samples used at LaRC and the NDE corrosion standards sent to Boeing, which are discussed below.

NDE Corrosion Standards: Four 1-inch by 1-inch corroded cold plate specimens were produced at NASA-LaRC, examined using CT radiography and supplied to Boeing Reusable Space Systems Division. Two of these specimens were corroded for 24 hours and two were corroded for 8 hours. The two exposure conditions were selected to produce a different distribution of sizes for the IGA present. The CT radiography results for each specimen were analyzed, and a mean maximum depth for each corrosion event was determined. The CT radiography images are shown in Figures 10-13. Each IGA event that was identified has been artificially shaded in order to present the IGA depth for each event on a single figure. Over 100 IGA events were identified for each standard; however, many events were found to coalesce, making it difficult to determine a specific depth. Therefore, only discreet events have been identified, encircled and numbered for each standard. These events (23 to 26 for each standard) are discreet events that were clearly identified using CT radiography. A table indicating the mean maximum depth of each identified IGA event, as determined using CT radiography, is provided for each standard (See Tables 3-6.). The CT radiography data was acquired in a slightly different manner for the two 8-hour specimens than for the two 24-hour specimens. The first slice for the 8 hour specimens was acquired at a shallower mean depth than was performed for the 24-hour specimens (0.0025 inch at 8 hours, 0.0035 inch at 24 hours). This resulted in corrosion depths that are different than for the 24-hour specimens. Since a direct comparison of results from CT radiography and a destructive examination was not conducted for the depths sampled for the 8 hour standards, a statistical analysis of these results is not available and no confidence interval data is provided for these standards. However, it is reasonable to believe that the range for a confidence interval for the data at 0.0075 inch would be at least as tight as that for 0.0065 inch at 24 hours and a similar argument can be made for comparing the 0.0095 and 0.0115-inch data to the 0.0085 and 0.0105-inch confidence intervals shown in Table 2.

Evaluation of NDE Methods:

Five NDE methods were chosen for evaluation (immersion ultrasonics, laser ultrasonics, eddy current, thermography, and digital radiography) because they are all capable of examining a complete avionics cold plate article. Three additional criteria were identified to determine the most appropriate NDE technique: (1) the ability to resolve corroded regions of material; (2) the ability to resolve discreet corrosion events; and (3) the capability of evaluating IGA penetration depth. For this evaluation 1-inch by 1-inch cold plate samples were prepared with one-half of the face sheet protected prior to exposing the samples to the electrolyte solution for 24 hours. Figure 14 shows a CT radiograph of such a specimen. The results from the five techniques being evaluated were compared to the CT radiography results to assess the capabilities of each technique. Of the five techniques examined, immersion ultrasonics has shown the best results with the capability of resolving discreet IGA events. A summary of each technique is listed below and a summary of the capabilities of each technique is listed in Table 7.

Immersion Ultrasonics: The immersion ultrasonics technique was able to detect discreet IGA events in corroded cold plate samples (Figure 15). Here, the darker regions throughout the corroded area of the cold plate specimen indicate IGA events. The ability to detect corrosion in cold plate samples can also be seen by comparing the ultrasonic response of specimens with and without IGA (Figure 16). These signals are representative of signals in regions where the face sheet is directly above a cooling hole; therefore, a post is not located directly below these portions of the face sheet. The time reference in this figure corresponds to the time of the reflection off the front surface of the face sheet, which is the large signal that appears to be nearly identical for the uncorroded and corroded points of the specimen. Following the signal due to the front surface reflection, the signal is representative of the reverberations of sound between the front and back surfaces. In regions where there is corrosion, these reverberations are significantly reduced.

To image the corrosion, the ultrasonic response between 1 and 2 microseconds was rectified and then integrated to give an output for each point on the specimen. From these outputs it is possible to create an image such as shown in Figure 15. Where there are posts below the face sheet, there are no reverberations, resulting in negligible signal, which produces round dark regions (See Figure 15.). Unlike the CT radiography technique, immersion ultrasonics does not provide a direct method for evaluating the penetration depth of the IGA events. However, by examining well-characterized samples, i.e. the NDE corrosion standards, it should be possible to determine the resolution for a particular immersion ultrasonics system. For this reason, the ability to determine IGA depth penetration has been listed as to be determined in Table 3.

Laser Ultrasonics: Results from the laser ultrasonics technique are shown in Figure 17. Here the corroded half of the specimen is clearly distinguished from the uncorroded half. However, this technique lacks the necessary fidelity to resolve individual IGA events. The laser ultrasonics technique generated modes that masked the echoes in the face sheet. While it may be possible to improve the results by applying a coating to the surface, this was not done in this case in an effort to maintain the integrity of the specimens. Application of the laser based ultrasonics technique is only desirable if it is not possible to perform immersion ultrasonics.

Eddy Current: The eddy current technique lacks sufficient spatial resolution for characterization of individual events (Figure 18). Here, the response from the corroded half of the specimen was clearly different than the response from the uncorroded half, but specific corrosion events could not be resolved. While it is possible to improve resolution by developing a smaller probe that would operate at higher frequencies, such an effort was beyond the scope of this work.

Thermography: Results from thermography were found to be very sensitive to surface or near surface conditions (Figure 19). It appears that this effect is due to the coating applied to the specimen, which is necessary to increase the surface emissivity. Since this technique is so sensitive to the near surface condition, it is not practical to use this method for this application.

Digital Radiography: Using the digital radiography technique, it was possible to observe indications of IGA events; however, another technique is required to improve sensitivity. Multiple images were acquired with different lines of sight through the specimen. An algorithm is being developed under another program that may make it possible to analyze these multiple images. Such an analysis may lead to an improved sensitivity of this technique in the future.

Summary

An accelerated laboratory method was developed that reproduces in-service IGA corrosion observed in avionic cold plates. This accelerated technique was used to produce NDE standards that contain IGA. CT radiography was successfully used to fully characterize NDE standards after detailed metallography was conducted to validate CT radiography results. Four corrosion standards were fabricated and characterized at NASA-LaRC. The standards were delivered to Boeing Reusable Space Systems Division to aid in developing new NDE methods for examining orbiter avionics cold plates. LaRC evaluated five NDE methods (immersion ultrasonics, laser ultrasonics, eddy current, thermography, and digital radiography) for detecting IGA in cold plates. Immersion ultrasonics was found to be the most promising technique for the inspection of IGA corrosion in cold plates; it has the resolution to delineate discrete corrosion events while being able to analyze large components.

Table 1. Cold Plate Specimens Prepared and Examined Using NDE and Destructive Techniques

	# of Samples
A. Corroded Specimens (total)	43
Coupled to 1-1/2-inch by 1-1/2-inch cathode	
8 hours	8
19 hours	12
24 hours	15
28 hours	3
Coupled to 2-1/4-inch by 2-1/4-inch cathode	
19 hours	5
B. Specimens destructively examined (total)	19
Coupled to 1-1/2-inch by 1-1/2-inch cathode	
8 hours	3
19 hours	3
24 hours	7
28 hours	3
Coupled to 2-1/4-inch by 2-1/4-inch cathode	
19 hours	3
C. Specimens examined by NDE techniques (total)	13
Coupled to 1-1/2-inch by 1-1/2-inch cathode	
8 hours	3
24 hours	10
D. Specimens/Standards supplied to Boeing (total)	5
Coupled to 1-1/2-inch by 1-1/2-inch cathode	
8 hours *	2
24 hours *	3

* - The 8-hour specimens and two of the 24-hour specimens were supplied as NDE standards.

Table 2. Confidence Intervals for Maximum IGA Depths Identified by CT Radiography for Cold Plate Specimens Exposed for 24 Hours

Mean max. depth from CT radiography (inch)	95% confidence interval (inch)
0.0045	--- *
0.0065	0.0058 – 0.0105
0.0085	0.0068 – 0.0106
0.0105	0.0086 – 0.0122
0.0125	--- *

* - Confidence intervals for 0.0045 and 0.0125-inch CT results could not be determined due to insufficient data correlating CT results with destructive evaluation.

Table 3. CT Radiography Results for Selected IGA Events for NDE Standard 17-24

Event *	CT result (in)	95% confidence interval (in)
1	0.0105	0.0086 – 0.0122
2	0.0105	0.0086 – 0.0122
3	0.0085	0.0068 – 0.0106
4	0.0105	0.0086 – 0.0122
5	0.0085	0.0068 – 0.0106
6	0.0105	0.0086 – 0.0122
7	0.0065	0.0058 – 0.0105
8	0.0065	0.0058 – 0.0105
9	0.0065	0.0058 – 0.0105
10	0.0065	0.0058 – 0.0105
11	0.0085	0.0068 – 0.0106
12	0.0065	0.0058 – 0.0105
13	0.0085	0.0068 – 0.0106
14	0.0105	0.0086 – 0.0122
15	0.0085	0.0068 – 0.0106
16	0.0065	0.0058 – 0.0105
17	0.0085	0.0068 – 0.0106
18	0.0105	0.0086 – 0.0122
19	0.0085	0.0068 – 0.0106
20	0.0085	0.0068 – 0.0106
21	0.0065	0.0058 – 0.0105
22	0.0045	---
23	0.0065	0.0058 – 0.0105
24	0.0065	0.0058 – 0.0105
25	0.0105	0.0086 – 0.0122
26	0.0125	---

* - Each event number is shown on Figure 10.

Table 4. CT Radiography Results for Selected IGA Events for NDE Standard 18-24

Event *	CT result (in)	95% confidence interval (in)
1	0.0085	0.0068 – 0.0106
2	0.0085	0.0068 – 0.0106
3	0.0085	0.0068 – 0.0106
4	0.0105	0.0086 – 0.0122
5	0.0065	0.0058 – 0.0105
6	0.0105	0.0086 – 0.0122
7	0.0105	0.0086 – 0.0122
8	0.0105	0.0086 – 0.0122
9	0.0065	0.0058 – 0.0105
10	0.0065	0.0058 – 0.0105
11	0.0045	---
12	0.0045	---
13	0.0125	---
14	0.0065	0.0058 – 0.0105
15	0.0085	0.0068 – 0.0106
16	0.0085	0.0068 – 0.0106
17	0.0105	0.0086 – 0.0122
18	0.0105	0.0086 – 0.0122
19	0.0105	0.0086 – 0.0122
20	0.0085	0.0068 – 0.0106
21	0.0105	0.0086 – 0.0122
22	0.0085	0.0068 – 0.0106
23	0.0065	0.0058 – 0.0105

* - Each event number is shown on Figure 11.

Table 5. CT Radiography Results for Selected IGA Events for NDE Standard 6-8

Event *	CT result (in)	Event *	CT result (in)
1	0.0095	14	0.0055
2	0.0075	15	0.0095
3	0.0035	16	0.0075
4	0.0055	17	0.0095
5	0.0035	18	0.0035
6	0.0075	19	0.0075
7	0.0075	20	0.0035
8	0.0075	21	0.0055
9	0.0055	22	0.0055
10	0.0055	23	0.0055
11	0.0075	24	0.0075
12	0.0055	25	0.0075
13	0.0075		

* - Each event number is shown on Figure 12.

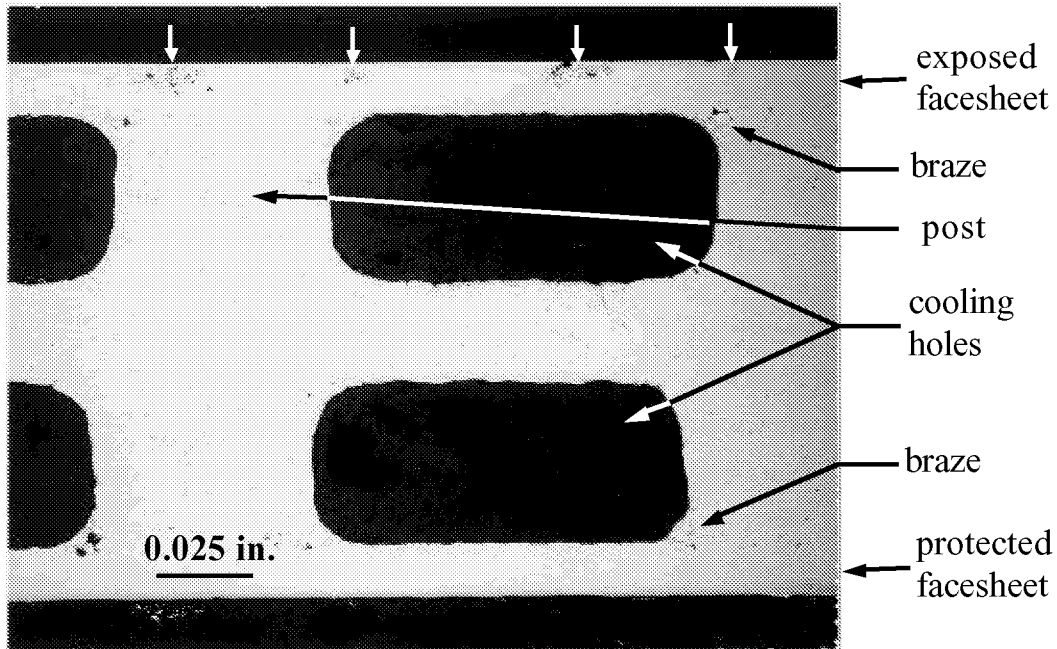
Table 6. CT Radiography Results for Selected IGA Events for NDE Standard 7-8

Event *	CT result (in)	Event *	CT result (in)
1	0.0055	14	0.0055
2	0.0075	15	0.0055
3	0.0055	16	0.0055
4	0.0055	17	0.0055
5	0.0075	18	0.0115
6	0.0075	19	0.0035
7	0.0075	20	0.0035
8	0.0035	21	0.0075
9	0.0035	22	0.0055
10	0.0055	23	0.0035
11	0.0055	24	0.0075
12	0.0055	25	0.0075
13	0.0035	26	0.0075

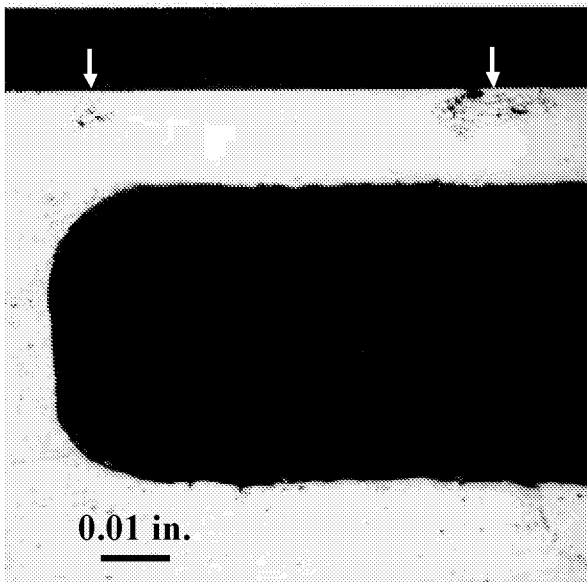
* - Each event number is shown on Figure 13.

Table 7. Evaluation of Technical Requirements for NDE Techniques Examined

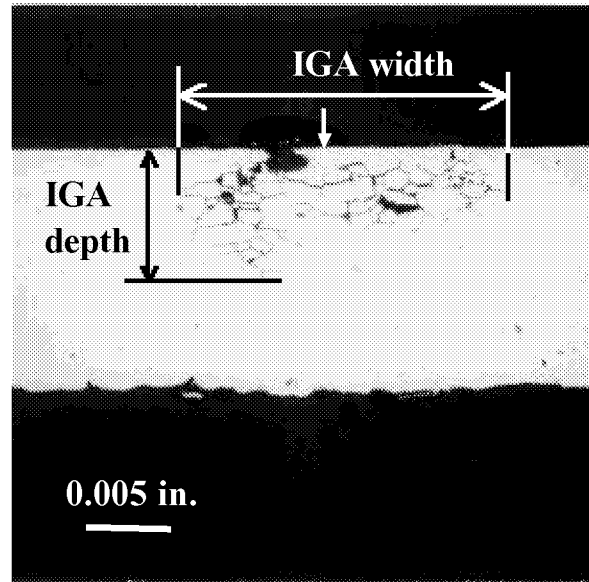
Technique	Resolve Corroded Regions	Resolve Discreet IGA Events	Determine IGA Penetration Depth
Immersion ultrasonics	✓	✓	TBD
Laser ultrasonics	✓	-	-
Eddy Current	✓	-	-
Thermography	✓	-	-
Digital Radiography	✓	✓	-



a)



b)



c)

Figures 1 a-c. Optical micrographs for three different magnification of IGA produced in a cold plate specimen in the laboratory. The 1-inch by 1-inch specimen was coupled to a 1-1/2-inch by 1-1/2-inch steel cathode and exposed to the electrolyte solution for 24 hours.

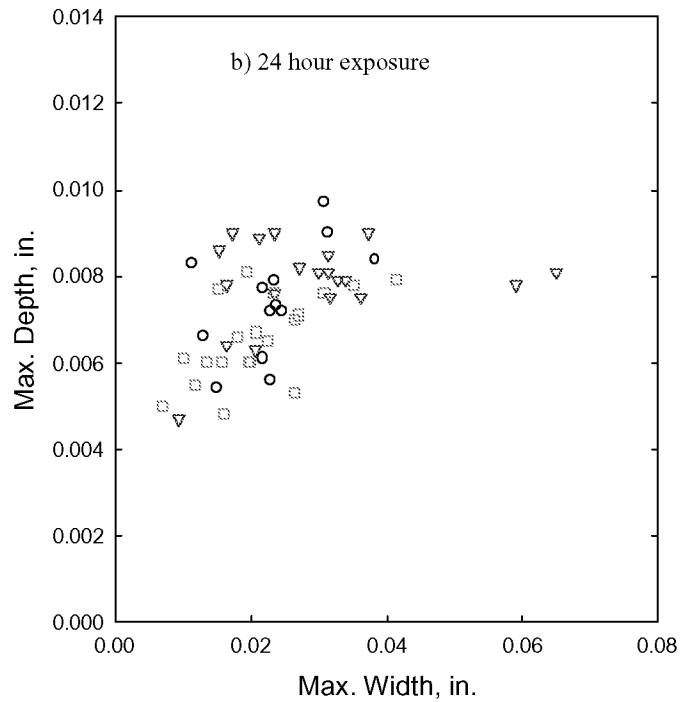
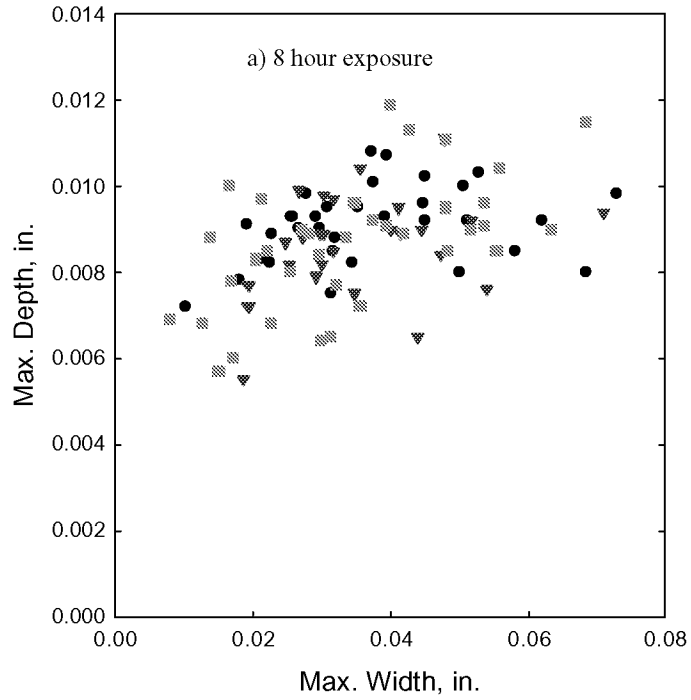
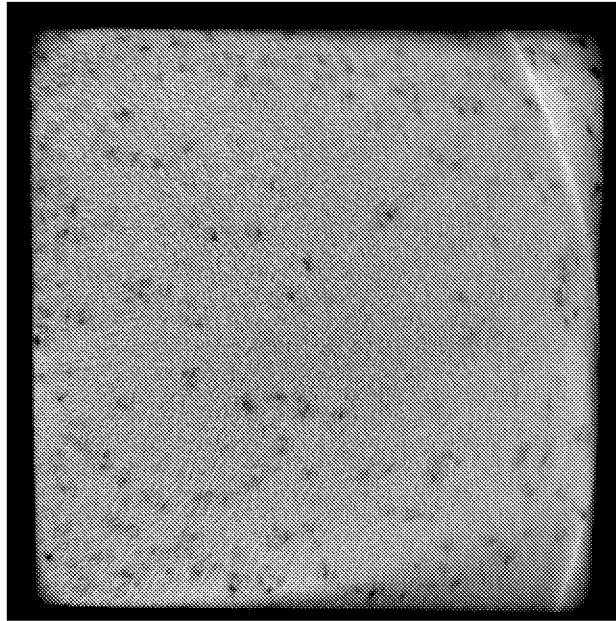
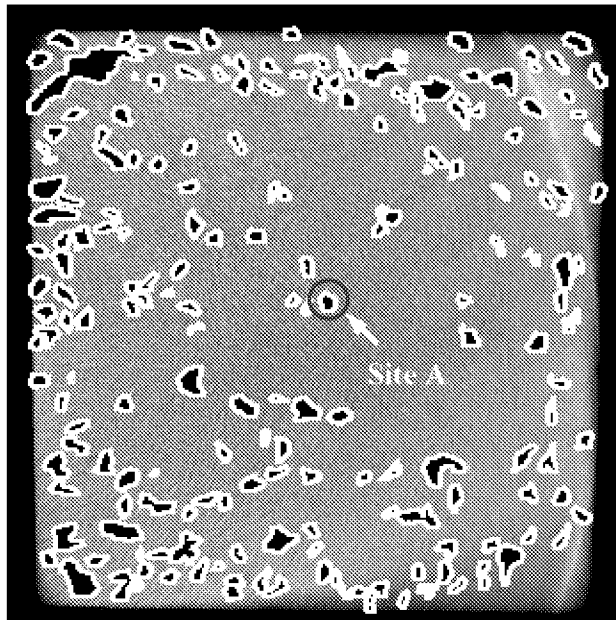


Figure 2. Plots showing depth versus width of IGA events measured using optical microscopy for cold plate specimens exposed to electrolyte. The different symbols represent results for different specimens examined.

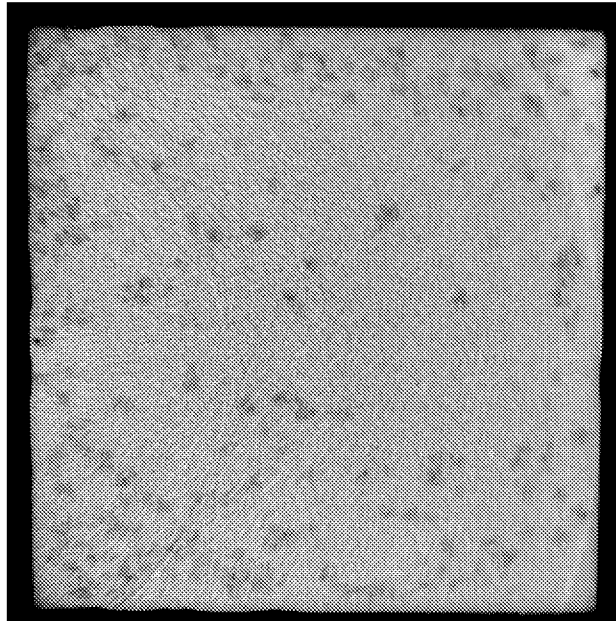


a)

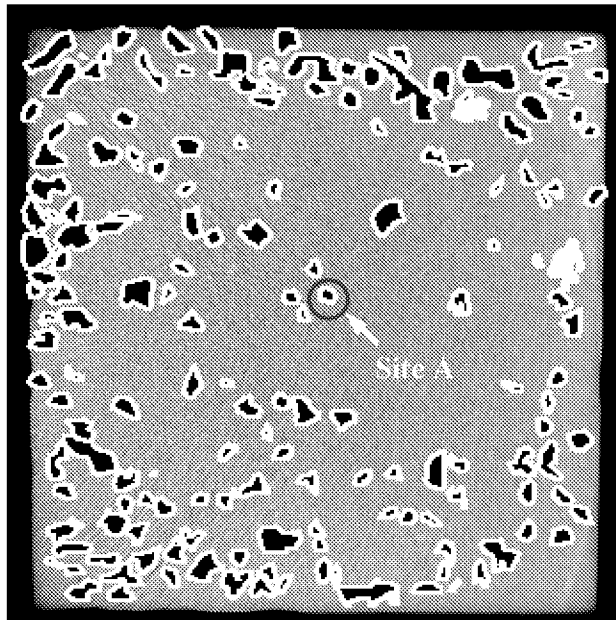


b)

Figure 3. CT radiography images for a 1-inch by 1-inch cold plate sample exposed to an electrolyte solution for 24 hours. The sensor head was located at a height that results in a mean sampling depth of 0.0035 inch. Figure 3a is the as acquired image while marks to identify IGA identified by CT radiography have been added to Figure 3b. One site has been identified for comparison with CT images acquired for several sampling depths (Identified as Site A in Figures 3b-7b.).

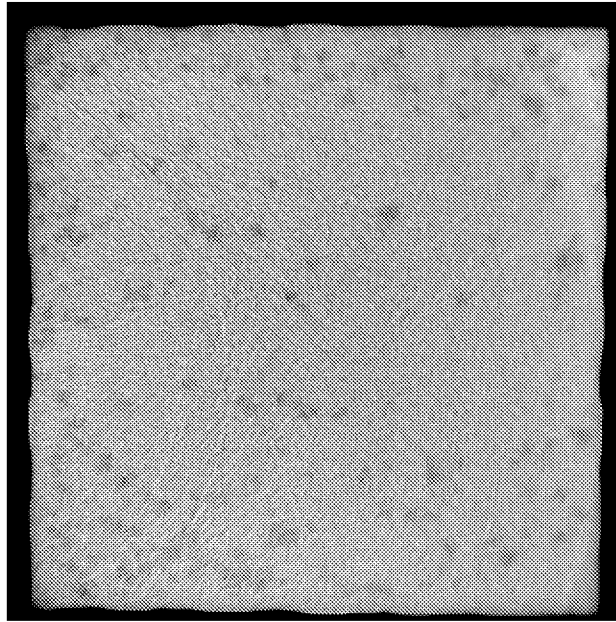


a)

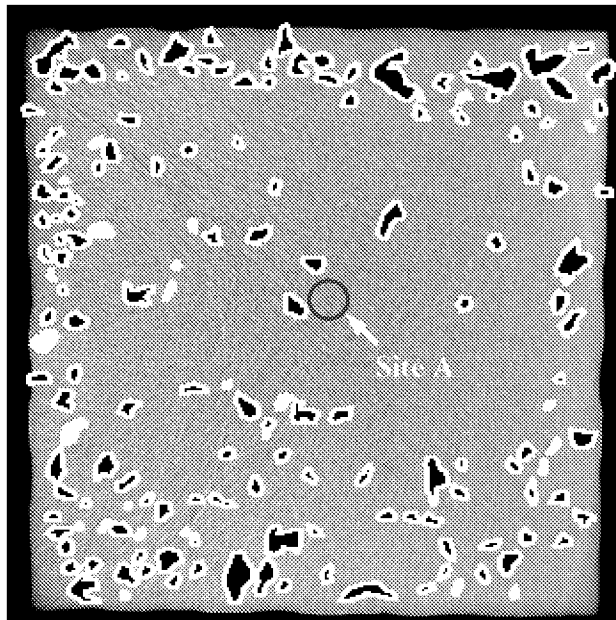


b)

Figure 4. CT radiography images for a 1-inch by 1-inch cold plate sample exposed to an electrolyte solution for 24 hours. The sensor head was located at a height that results in a mean sampling depth of 0.0055 inch. Figure 4a is the as acquired image while marks to identify IGA identified by CT radiography have been added to Figure 4b. One site has been identified for comparison with CT images acquired for several sampling depths (Identified as Site A in Figures 3b-7b.).

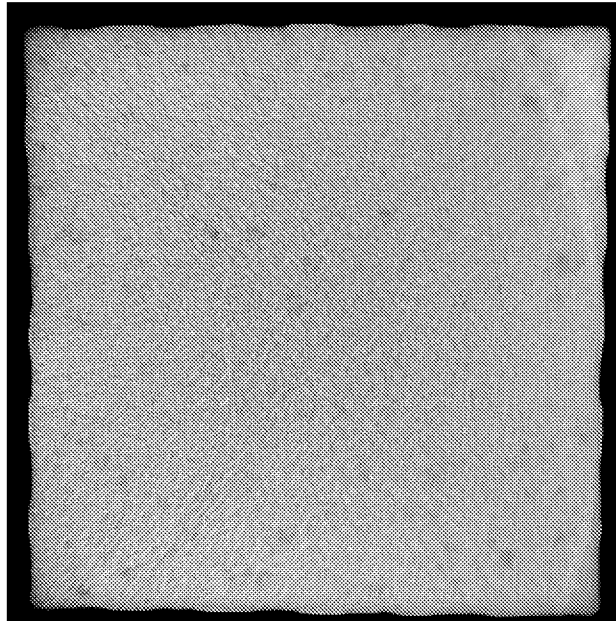


a)

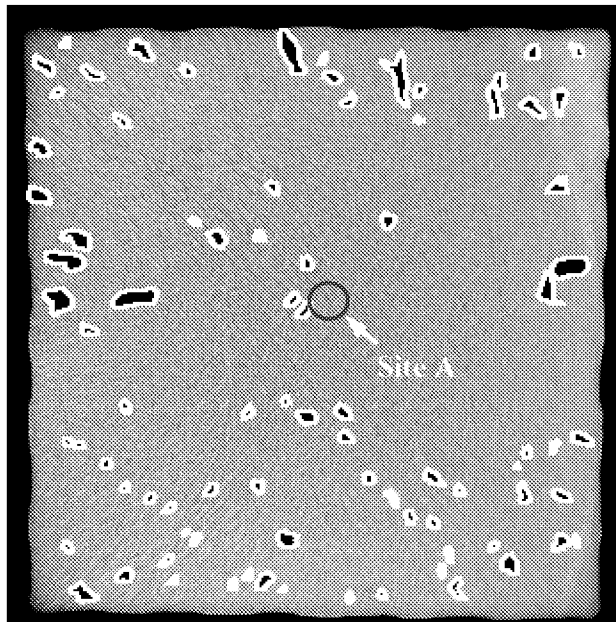


b)

Figure 5. CT radiography images for a 1-inch by 1-inch cold plate sample exposed to an electrolyte solution for 24 hours. The sensor head was located at a height that results in a mean sampling depth of 0.0075 inch. Figure 5a is the as acquired image while marks to identify IGA identified by CT radiography have been added to Figure 5b. One site has been identified for comparison with CT images acquired for several sampling depths (Identified as Site A in Figures 3b-7b).

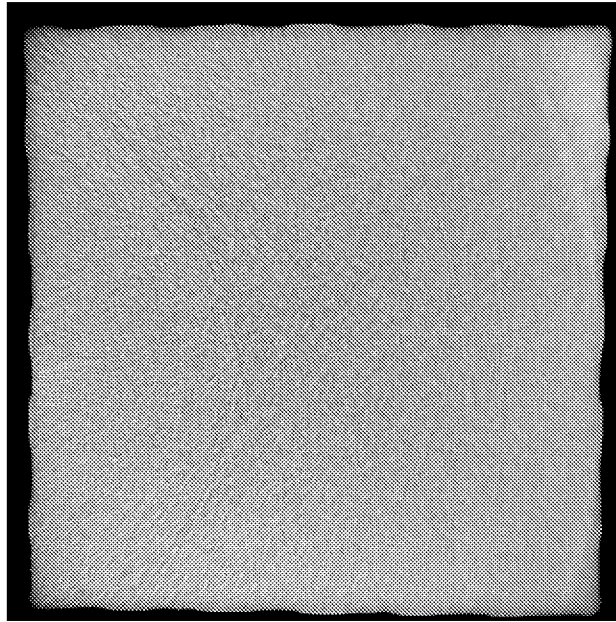


a)

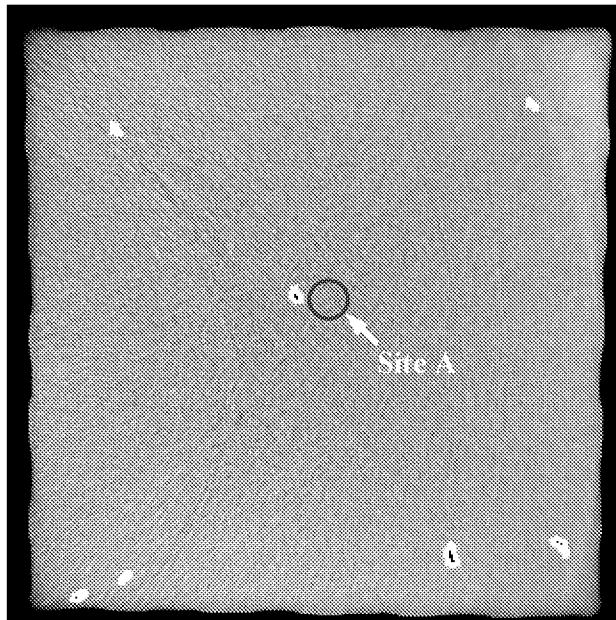


b)

Figure 6. CT radiography images for a 1-inch by 1-inch cold plate sample exposed to an electrolyte solution for 24 hours. The sensor head was located at a height that results in a mean sampling depth of 0.0095 inch. Figure 6a is the as acquired image while marks to identify IGA identified by CT radiography have been added to Figure 6b. One site has been identified for comparison with CT images acquired for several sampling depths (Identified as Site A in Figures 3b-7b.).



a)



b)

Figure 7. CT radiography images for a 1-inch by 1-inch cold plate sample exposed to an electrolyte solution for 24 hours. The sensor head was located at a height that results in a mean sampling depth of 0.0115 inch. Figure 7a is the as acquired image while marks to identify IGA identified by CT radiography have been added to Figure 7b. One site has been identified for comparison with CT images acquired for several sampling depths (Identified as Site A in Figures 3b-7b.).

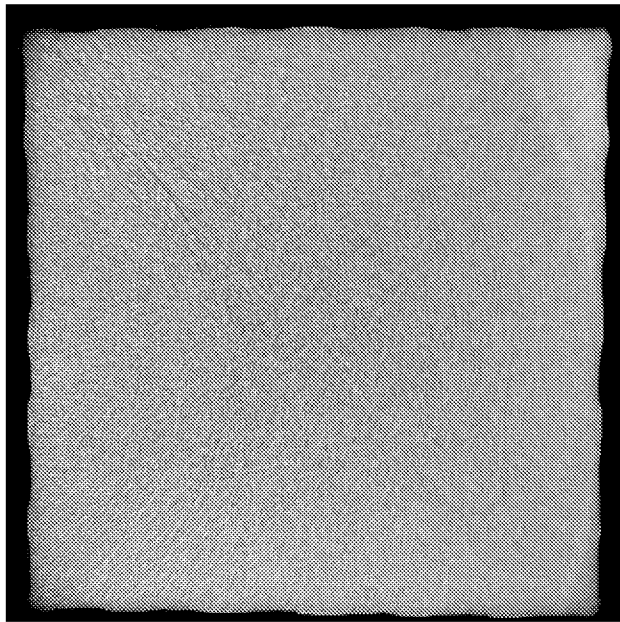


Figure 8. CT radiography image for a 1-inch by 1-inch cold plate sample exposed to an electrolyte solution for 24 hours. The sensor head was located at a height that results in a mean sampling depth of 0.0135 inch. No IGA was identified at this sampling depth.

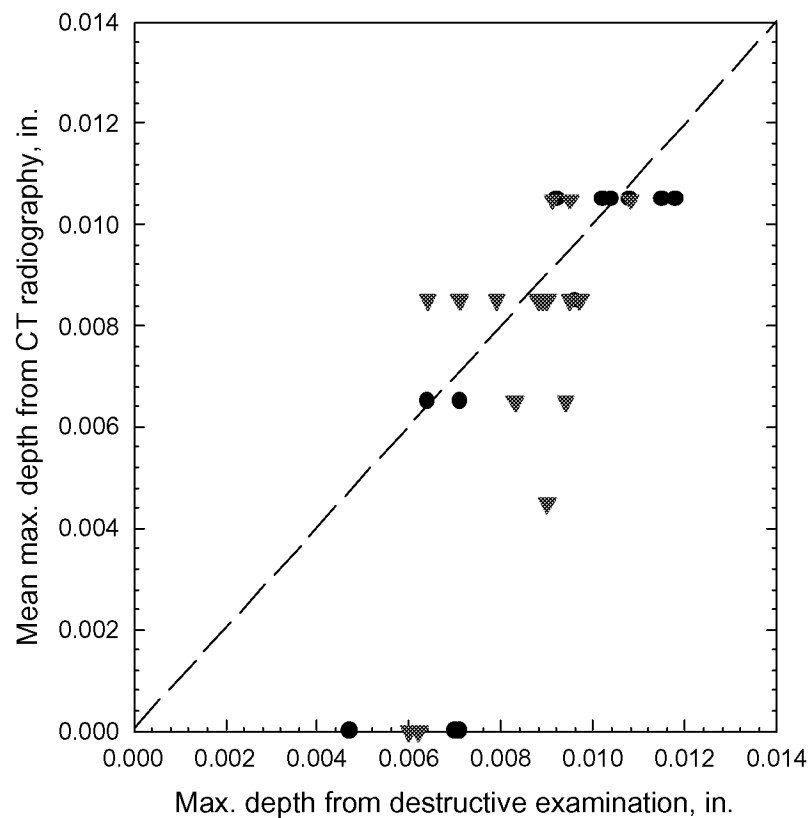


Figure 9. Plot of mean maximum depth of IGA events as determined by CT radiography versus maximum depth of the same IGA events as determined by a destructive examination. The two symbols are used to distinguish two cold plate samples. Both samples were exposed to an electrolyte solution for 24 hours while coupled to a steel cathode.

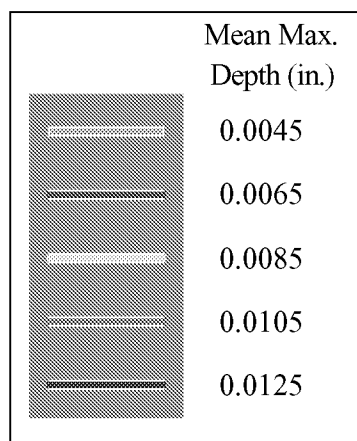
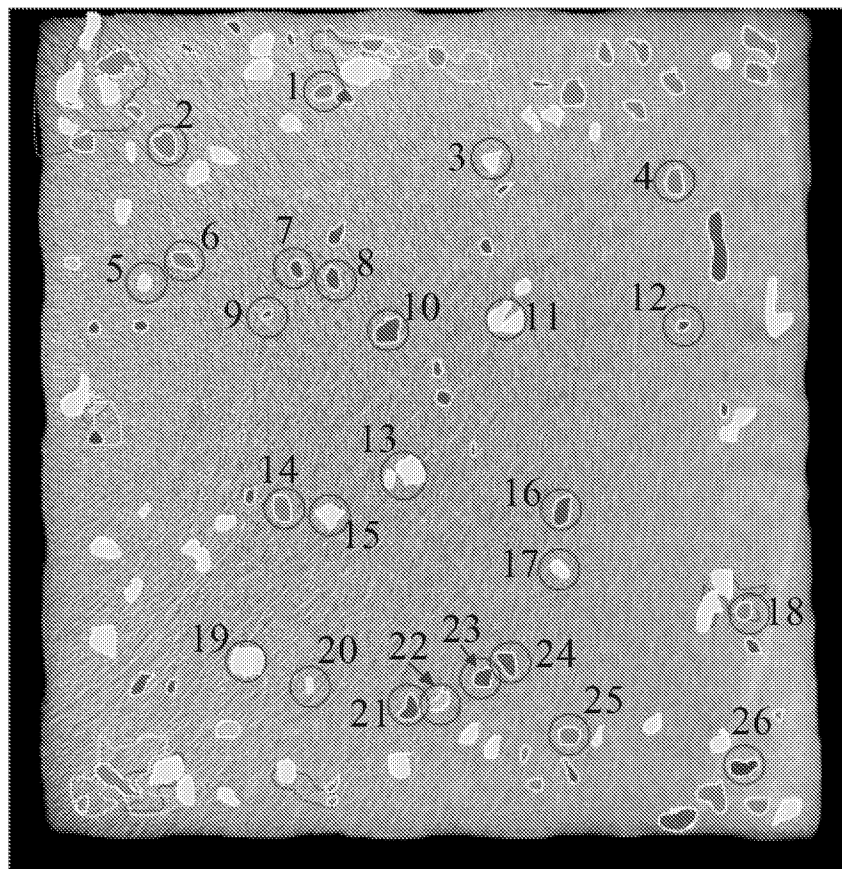


Figure 10. CT radiography image for NDE Standard 17-24. Specimen was exposed to electrolyte for 24 hours. A list of results for each event is given in Table 3.

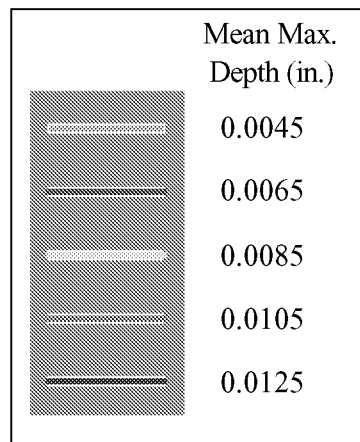
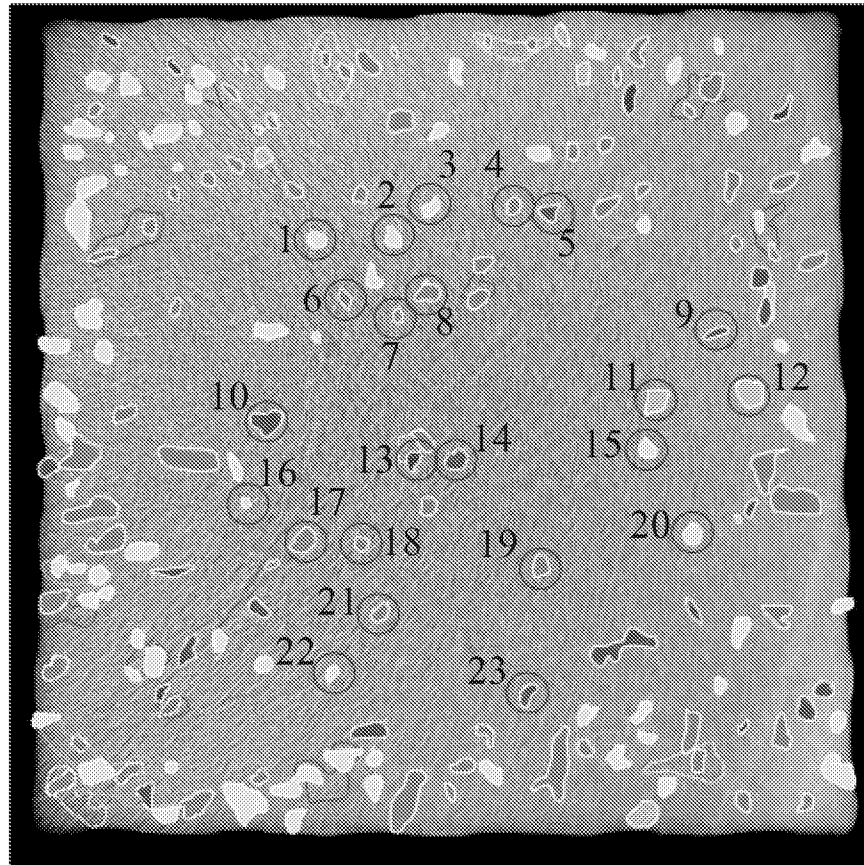


Figure 11. CT radiography image for NDE Standard 18-24. Specimen was exposed to electrolyte for 24 hours. A list of results for each event is given in Table 4.

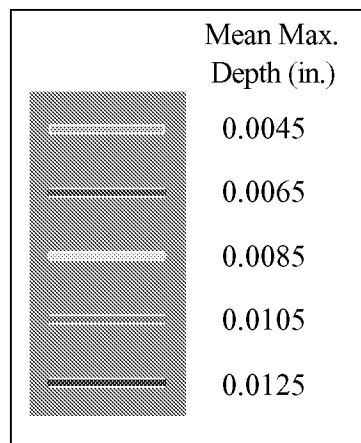
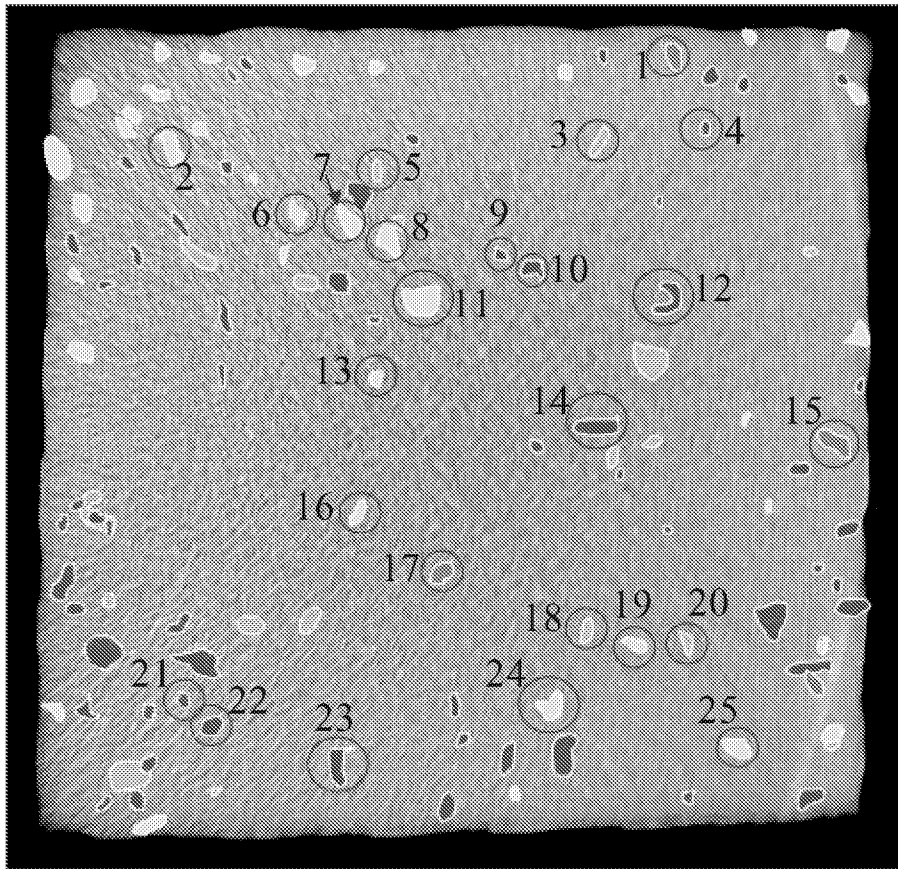


Figure 12. CT radiography image for NDE Standard 6-8. Specimen was exposed to electrolyte for 8 hours. A list of results for each event is given in Table 5.

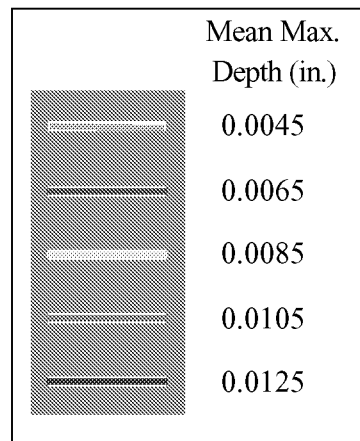
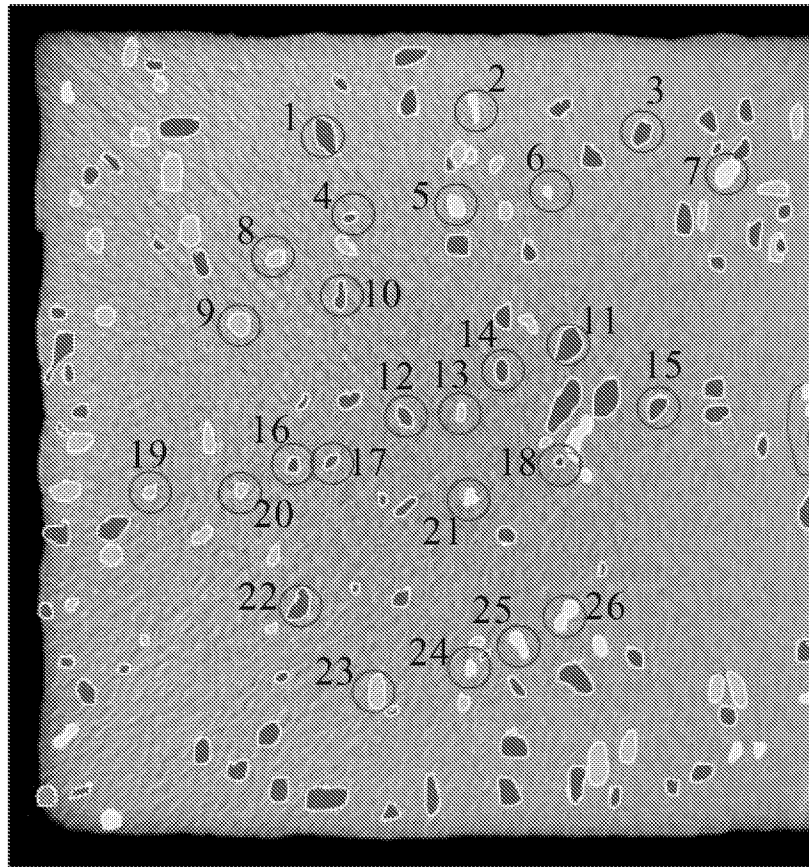


Figure 13. CT radiography image for NDE Standard 7-8. Specimen was exposed to electrolyte for 8 hours. A list of results for each event is given in Table 6.

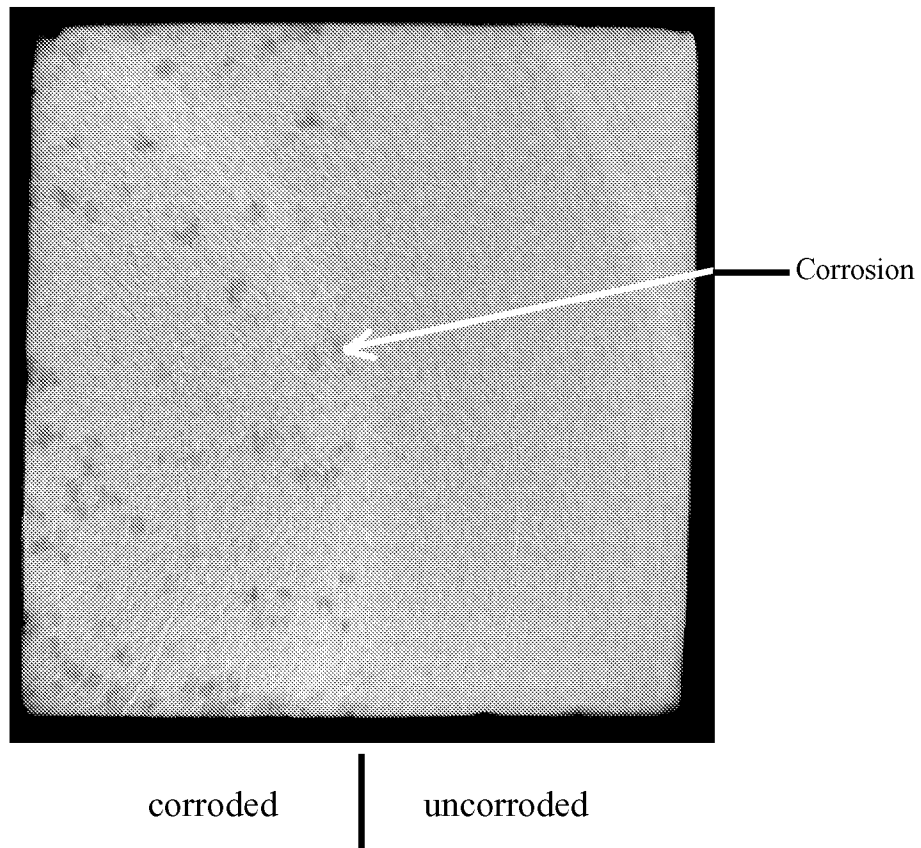


Figure 14. CT radiography results for a 1-inch by 1-inch corroded cold plate sample. The right half of the specimen was coated with wax to prevent corrosion, while the left half of the specimen was exposed to an electrolyte solution for 24 hours while coupled to a steel cathode. The sensor position results in a mean sampling depth of 0.0055 inch.

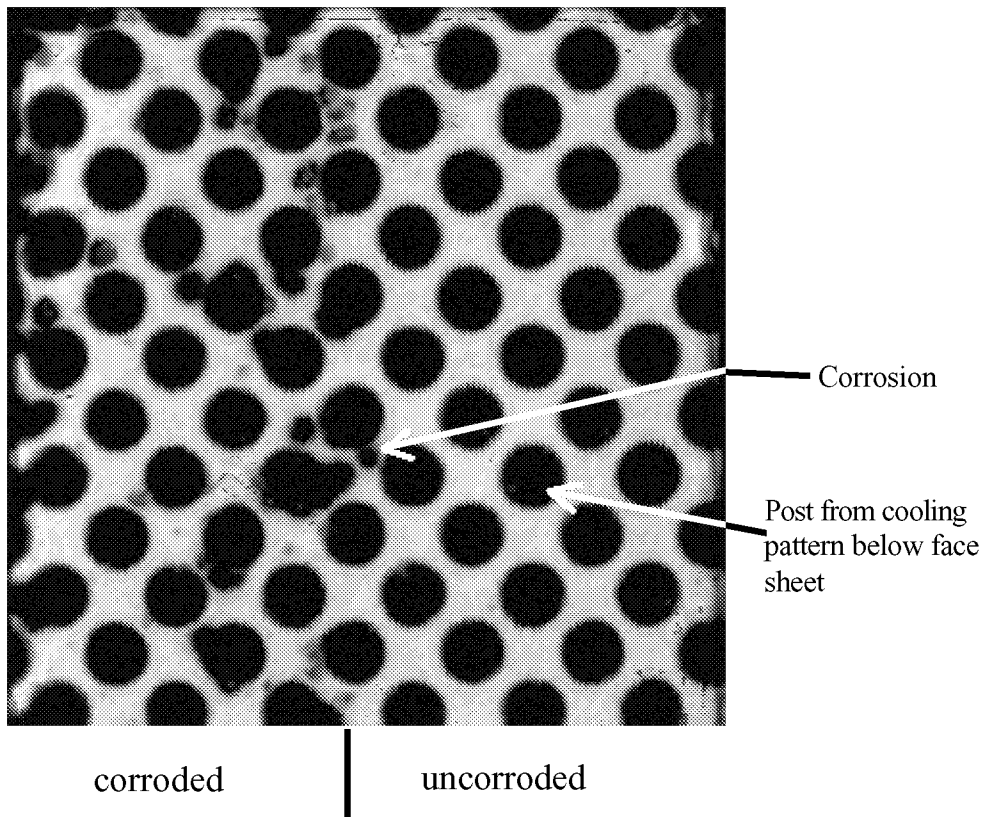


Figure 15. Immersion ultrasonic results for a 1-inch by 1-inch corroded cold plate sample. The right half of the specimen was coated with wax to prevent corrosion, while the left half of the specimen was exposed to an electrolyte solution for 24 hours while coupled to a steel cathode.

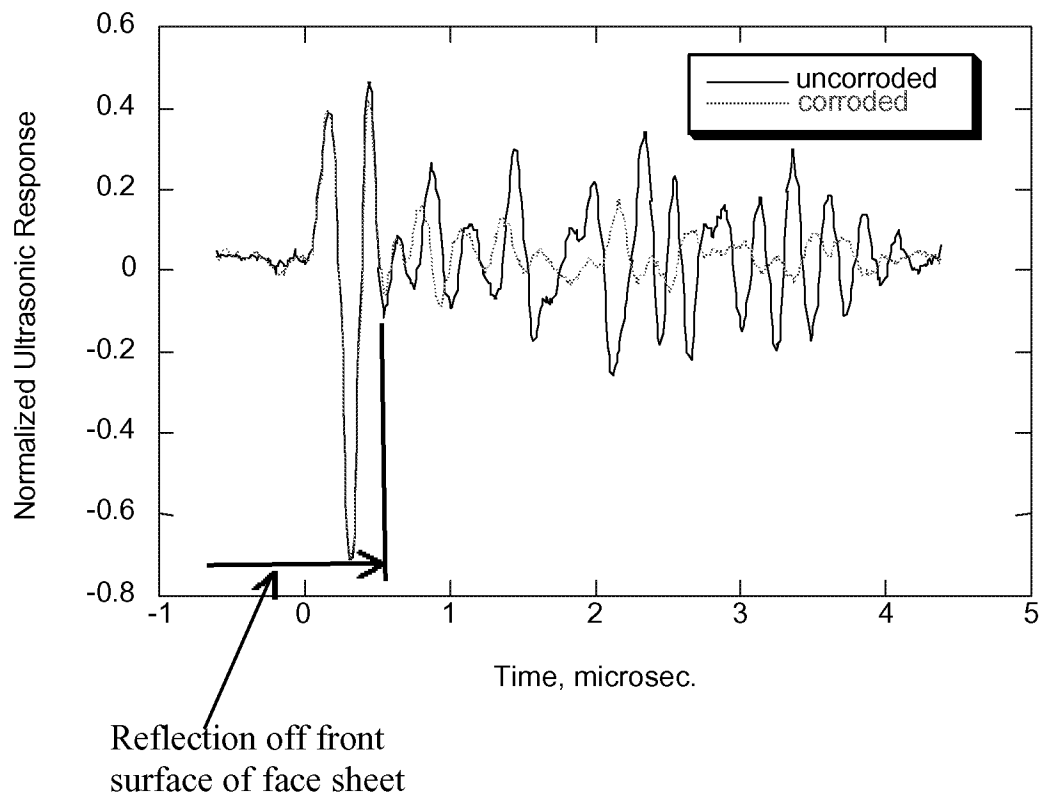


Figure 16. Ultrasonic response for immersion ultrasonic analysis for uncorroded and corroded cold plate samples. The corroded specimen was exposed to an electrolyte solution for 24 hours while coupled to a steel cathode.

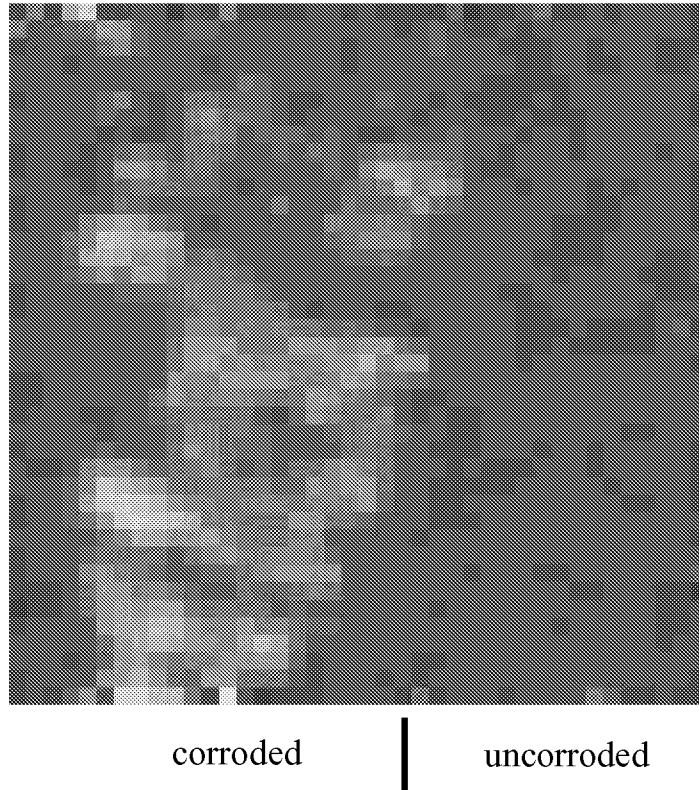
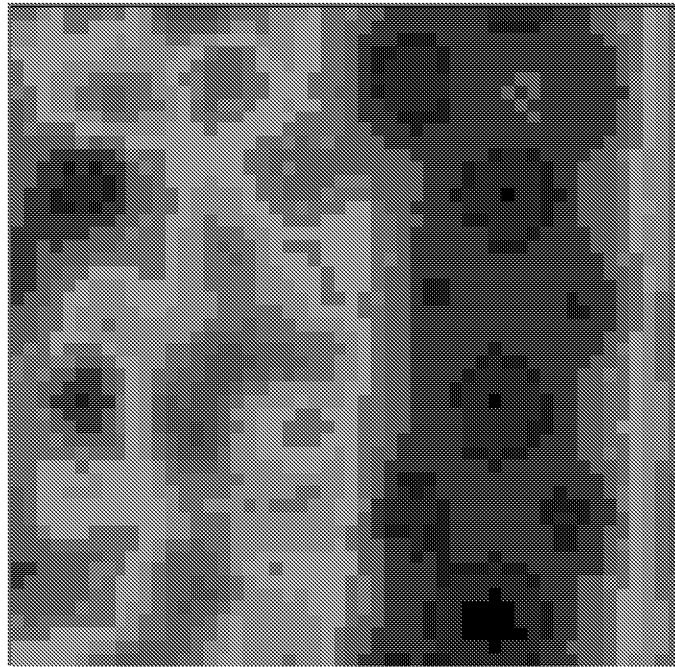


Figure 17. Laser ultrasonic results for a 1-inch by 1-inch corroded cold plate sample. The right half of the specimen was coated with wax to prevent corrosion, while the left half of the specimen was exposed to an electrolyte solution for 24 hours while coupled to a steel cathode.



corroded

uncorroded

Figure 18. Eddy current results for a $\frac{1}{4}$ inch by $\frac{1}{4}$ inch segment of a corroded cold plate sample. The right half of the specimen was coated with wax to prevent corrosion, while the left half of the specimen was exposed to an electrolyte solution for 24 hours while coupled to a steel cathode.

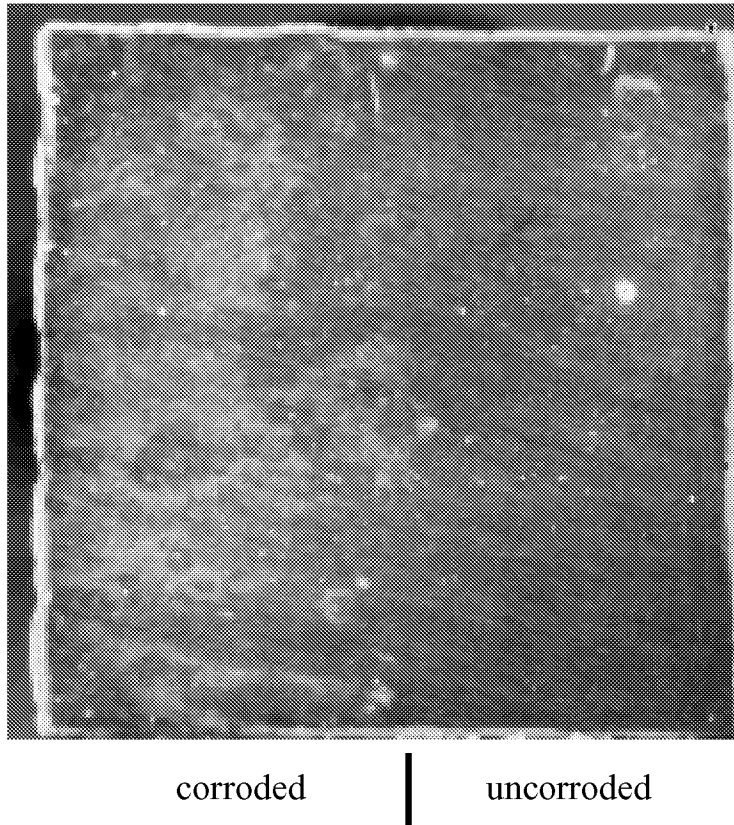


Figure 19. Thermography results for a 1-inch by 1-inch corroded cold plate sample. The right half of the specimen was coated with wax to prevent corrosion, while the left half of the specimen was exposed to an electrolyte solution for 24 hours while coupled to a steel cathode.

REPORT DOCUMENTATION PAGE			Form Approved OMB No. 0704-0188	
Public reporting burden for this collection of information is estimated to average 1 hour per response, including the time for reviewing instructions, searching existing data sources, gathering and maintaining the data needed, and completing and reviewing the collection of information. Send comments regarding this burden estimate or any other aspect of this collection of information, including suggestions for reducing this burden, to Washington Headquarters Services, Directorate for Information Operations and Reports, 1215 Jefferson Davis Highway, Suite 1204, Arlington, VA 22202-4302, and to the Office of Management and Budget, Paperwork Reduction Project (0704-0188), Washington, DC 20503.				
1. AGENCY USE ONLY (Leave blank)		2. REPORT DATE January 2002	3. REPORT TYPE AND DATES COVERED Technical Memorandum	
4. TITLE AND SUBTITLE Orbiter Cold Plate Intergranular Corrosion: Development of NDE Standards and Assessment of NDE Methods			5. FUNDING NUMBERS WU 706-62-31-01	
6. AUTHOR(S) Stephen W. Smith, William P. Winfree, and Robert S. Piascik				
7. PERFORMING ORGANIZATION NAME(S) AND ADDRESS(ES) NASA Langley Research Center Hampton, VA 23681-2199			8. PERFORMING ORGANIZATION REPORT NUMBER L-18144	
9. SPONSORING/MONITORING AGENCY NAME(S) AND ADDRESS(ES) National Aeronautics and Space Administration Washington, DC 20546-0001			10. SPONSORING/MONITORING AGENCY REPORT NUMBER NASA/TM-2002-211420	
11. SUPPLEMENTARY NOTES				
12a. DISTRIBUTION/AVAILABILITY STATEMENT Unclassified-Unlimited Subject Category 26 Distribution: Standard Availability: NASA CASI (301) 621-0390			12b. DISTRIBUTION CODE	
13. ABSTRACT (Maximum 200 words) During pre-servicing of a space shuttle (orbiter vehicle, OV-102), helium leak detection of an avionics cold plate identified a leak located in the face sheet oriented towards the support shelf. Subsequent destructive examination of the leaking cold plate revealed that intergranular corrosion had penetrated the 0.017-inch thick aluminum (AA6061) face sheet. The intergranular attack (IGA) was likely caused by an aggressive crevice environment created by condensation of water vapor between the cold plate and support shelf. Face sheet susceptibility to IGA is a result of the brazing process used in the fabrication of the cold plates. Cold plate components were brazed at 1000°F followed by a slow cooling process to avoid distortion of the bonded cold plate. The slow cool process caused excessive grain boundary precipitation resulting in a material that is susceptible to IGA. The objectives of this work are as follows: <ol style="list-style-type: none"> (1) Develop first-of-a-kind NDE standards that contain IGA identical to that found in the orbiter cold plates. (2) Assess advanced NDE techniques for corrosion detection and recommend methods for cold plate examination. This report documents the results of work performed at LaRC to fulfill these objectives.				
14. SUBJECT TERMS NDE inspection; corrosion detection; intergranular corrosion; intergranular attack			15. NUMBER OF PAGES 36	
			16. PRICE CODE A03	
17. SECURITY CLASSIFICATION OF REPORT Unclassified	18. SECURITY CLASSIFICATION OF THIS PAGE Unclassified	19. SECURITY CLASSIFICATION OF ABSTRACT Unclassified	20. LIMITATION OF ABSTRACT UL	